

DESY SUMMER STUDENT PROJECT



Setup for Electron Diffraction off Controlled Molecules

Florian Friedrich

(DESY Summer Student 2015)

Area of research:

Photon Science, Molecular Physics

Time frame:

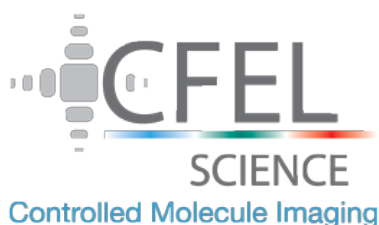
July 21 - September 10, 2015

Author:

Florian Friedrich
Heidelberg University
Im Neuenheimer Feld 227
69120 Heidelberg, Germany

Supervisor:

Joss Wiese
Deutsches Elektronen Synchrotron (DESY)
Center for Free-Electron Laser Science (CFEL)
Controlled Molecule Imaging (CMI)
Notkestr. 85
22607 Hamburg, Germany



Contents

1	Introduction	3
2	Setup	3
3	VMI Spectrometer	7
3.1	Calibration	7
3.2	Spatial Imaging	9
3.3	Velocity Map Imaging	9
4	Measurement	10
4.1	Time Offset	10
4.2	Beam Profile	11
5	Conclusion	12

1 Introduction

Electron diffraction off gas-phase molecules is an upcoming approach to image structural features of isolated molecules. Thus, this technique provides scope for the investigation of innermost properties and dynamics of molecules.

In the experimental setup presented here, cool gas-phase samples were created via supersonic co-expansion with helium through a pulsed valve. Passing a deflector the molecules with the lowest rotation energy level became selected and separated from the helium. The electric field of an intense pulsed laser aligned the molecules adiabatically. There were two ways to probe the molecules. A femtosecond laser was used to examine the molecular alignment via strong-field ionization (Coulomb explosion). The objective was to get structural information via diffraction of a pulsed electron beam. In both cases the probe laser or the electron beam respectively crossed the molecular beam inside a VMI spectrometer.

There are successful examples of molecular diffraction images taken with ultrafast electron pulses [1]. This experimental setup has the purpose of combining strong alignment and high repetition rates. In a similar setup strong laser alignment and mixed-field orientation at kHz repetition rate could be demonstrated [2]. After adding an electron gun [3] the current objective is to calibrate the setup and record first electron diffraction images.



Figure 1: Picture of the setup

2 Setup

The experimental setup consisted of a vacuum chamber with three compartments: a first one to create a beam of cold molecules, a second to deflect the beam and a third with a Velocity Map Imaging (VMI) spectrometer and detector. An increasing vacuum is

achieved by differential pumping. Figure 1 and Figure 2 show a picture and a schematic representation of a previous setup, where no electron gun was implemented and the VMI spectrometer was oriented parallel to the molecular beam. For this measurement an electron gun was added and the VMI spectrometer as well as the detector were oriented perpendicular to the molecular beam.

The molecule of interest, 2,5-Diiodobenzonitrile (DIBN) (Figure 3), was seeded in helium as carrier gas with a pressure of 90 bar and co-expanded into a vacuum of $\sim 10^{-7}$ mbar. Hereby the transition through an Even-Lavie valve produced a supersonic expansion and cooling of the molecules down to around 1 K. Upon passage through the valve's nozzle collisions between the sample and the helium occurred, so that the internal energy (vibration and rotation) of the sample was transformed adiabatically to transversal kinetic energy of the helium atoms. Rotational states, typically with quantum numbers $J = 0..20$, were still occupied, while only the first electronic state and a few (one to three) vibrational states kept occupied. The longitudinal velocity along the propagation direction of the molecular beam was around 1 km/s.

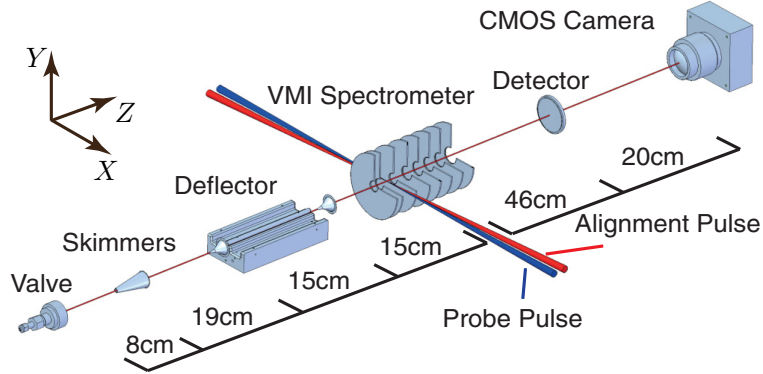


Figure 2: Experimental setup

Multiple skimmers were used to shape the molecular beam in order to cut away molecules with higher transversal velocity. The second vacuum chamber had a pressure of $\sim 10^{-9}$ mbar and included the deflector (Figure 4), where the molecules were separated via the DC Stark effect. The Stark effect describes deflection of molecules in static electric fields by a shift of the energy levels, analog to the Zeeman effect in a static magnetic field. The deflection corresponds to the effective dipole moment $\vec{\mu}_{eff}$ of a molecule. The electric field \vec{E} has to be strongly inhomogeneous to get good deflection and the horizontal field lines are needed to avoid aberration. The two poles of the deflector had a potential difference of 10 kV, while the electric field inside the deflector varied from 60 kV/cm to 120 kV/cm (Figure 4). Since the interaction energy of a molecule in a static electric field is $V = -\vec{\mu} \cdot \vec{E}$, the molecule experiences the force $\vec{F} = -\vec{\mu}_{eff}(\vec{E}) \cdot \nabla(\vec{E})$.

Deflection was important to select the molecules with the lowest rotational energy level because they were better to align. After being dispersed the molecular beam passed a second skimmer, which is essential to cut away most of the helium atoms, because they don't show deflection ($\vec{\mu}_{eff} = 0$).

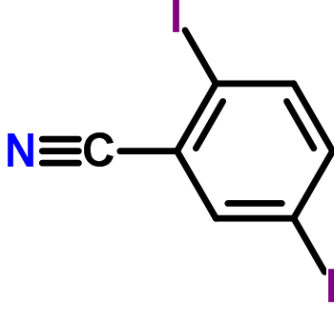


Figure 3: 2,5-Diiodobenzonitrile

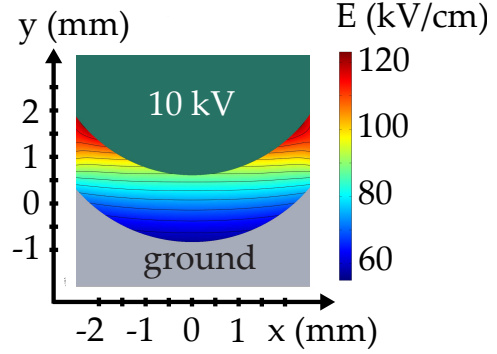


Figure 4: Electric field inside deflector

The third compartment has only $\sim 9 \cdot 10^{-10}$ mbar containing the VMI spectrometer. An alignment laser with 500 ps pulse duration and a wavelength of 800 nm, ~ 70 nm bandwidth, was used to align the molecules according to the laser's electrical field. Since the rotational motion of the sample molecules is several orders of magnitude slower than the oscillating electrical field of the alignment laser, the dipole moment has no effect of aligning the molecule. Instead, the polarizability tensor describes the interaction with the oscillating electric field of the laser. The larger the polarization the stronger is the interaction, while the molecule's axis with highest polarization goes through both iodine atoms. Pulses with high intensity were required [4], because the AC (second order) Stark effect is small compared to the DC (first order) Stark effect. The pulsed alignment laser had a repetition rate of 1 kHz and a pulse intensity of $3.2 \cdot 10^{11}$ W/cm². The intensity can be calculated with the pulse energy P_{Pulse} , the pulse duration $FWHM_t$ and the standard deviations σ_i of the laser profile assuming Gaussian profiles in time and two-dimensional space:

$$I = \frac{P_{Pulse}}{2\pi \cdot FWHM_t \cdot \sigma_x \cdot \sigma_y} \quad (1)$$

We used quasi-adiabatic alignment with laser pulses in the same regime as the rotational period of the molecules. Therefore the molecules reached maximal alignment during the interaction with the laser and no energy was left in the system after the laser pulse. One dimensional alignment was archived using a linear polarized laser. The molecules had just the most polarizable axis fixed in space. Two orientations (right side up or upside down) and rotation along the axis could still occur. Orientation was not used for this measurement but could had obtained by adding a static electric field of the VMI electrodes.

A probe laser with $\lambda = 800 \pm 35$ nm and $2.5 \cdot 10^{14}$ W/cm² peak intensity was used to examine the degree of alignment. The intensity were high enough to ionize the hit molecules via strong field ionization. The repulsive Coulomb force of the positive charges

inside the molecules let the molecule break apart (Coulomb explosion). We assume that the I^+ ion fled apart of the molecule along the I-I-axis of the molecule, because the remaining iodine atom had induced the most charge. As the I-I axis also represented the alignment axis of the sample, the direction of the I^+ ion on a velocity map showed the direction of the alignment axis of the whole molecule.

When good alignment was achieved, the goal was to investigate the structure of the molecule by measuring electron diffraction. Hereby, one obtains more structural information for aligned molecules. Another laser with 400 ps pulse duration and wavelengths in the range of 400 ± 10 nm produced electrons on a copper cathode for the electron beam. The electrons were accelerated upwards, focused via electrostatic lenses and diffracted off the aligned molecules.

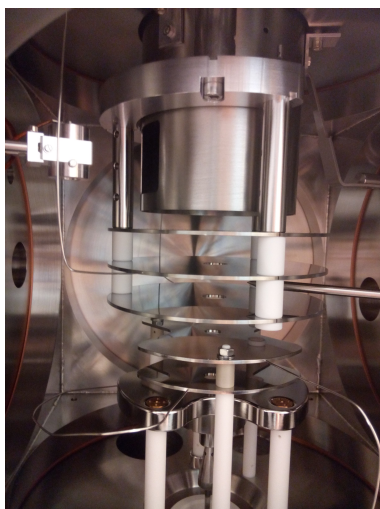


Figure 5: Picture of VMI spectrometer and electron gun. Lower three plates: copper cathode and electrostatic lenses, upper three plates: VMI electrodes.

The VMI spectrometer shown in Figure 5 basically consisted of two sets of ring-shaped electrodes, one for the electron gun which acted like an electron lens and a second one for imaging purposes. The laser hit the cathode at the bottom of the spectrometer to photo-emit electrons via two-photon absorption. Two photons had enough energy to surpass the 4.7 eV work function of copper. The typical operation voltage of the cathode was -25 kV. The electrons were focused on the detector by the first plate with a voltage of -22 kV while being accelerated upward to the second grounded plate. Focusing the electron beam was important to combine a sharp diffraction image and a long coherence length of the electron beam.

The upper three plates belonged to the VMI spectrometer. The molecular beam passed through horizontally in between the first and second plates of the VMI which had voltages in the range of 2 to 4 kV while the third imaging VMI plate was again grounded. Details follow in the next chapter.

A chevron-stacked microchannel plate (MCP) and a phosphor screen detected the diffracted

electrons. A CMOS camera took single-shot images of the phosphor screen with 1 kHz readout frequency. The structure of the molecule can be determined by comparing the diffraction pattern of the experiment with a simulation of the expected structure. If both patterns do not fit together, an algorithm modifies the supposed structure iteratively until measurement and simulation show the same diffraction and the structure is found. Here alignment is important to increase the contrast of the picture and to improve the results of the holography.

3 VMI Spectrometer

The detector can be run in two different ways. Ions can be pictured according to their actual position in the system of the molecular beam using spatial imaging mode. Moreover the ions' initial velocities can be pictured with velocity map imaging [5]. Changing the voltage of the two VMI plates allowed to switch easily between both modes.

3.1 Calibration

In Figure 6 a picture was taken to find the conversion factor of 9 pixel/mm to translate the pixel position on the phosphor screen to a distance in mm. The bright spot in the lower left corner belongs to a LED which was used to distinguish automatically measurements of the molecular beam and the background.

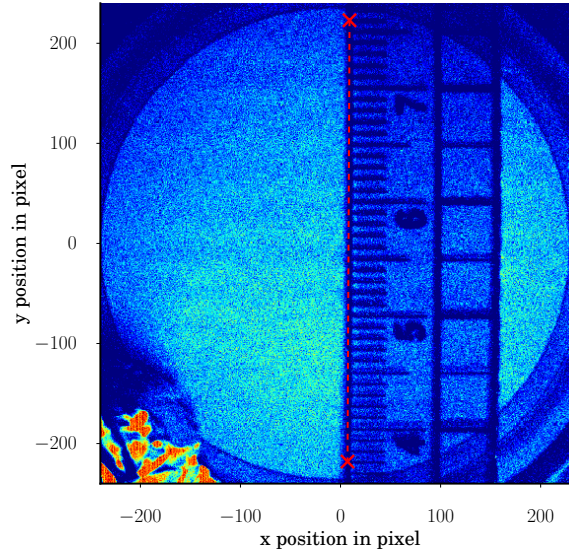


Figure 6: Calibration measurement of camera

Moreover there was an additional magnification inside our VMI spectrometer for both types of imaging. This factor was determined by the ion trajectory simulation program SIMION (Version 8.1) [6]. The magnification factor depends on the imaging mode and

for velocity mapping also on the voltage of the VMI plates as one can see at Table 1. First of all, the best setting for the second VMI plate was simulated to achieve perfect spatial and velocity resolution for a given voltage of 3 kV and 4 kV of the first VMI plate. Using both voltages and a calibration particle (mass = 53 u, charge = 1 e), following magnification factors and times of flight (TOF) were simulated. Negative magnification factors stand for an upside down projection.

Imaging	V_{VMI1} [V]	V_{VMI2} [V]	magnification factor	$\text{TOF}_{m=53u}$ [μs]
Spatial	4000	3580	-3.499 ± 0.002	2.287
Velocity	4000	2606	2.275 ± 0.001	2.068
Spatial	3000	2685	-3.507 ± 0.005	2.641
Velocity	3000	1963	2.612 ± 0.001	2.388

Table 1: Magnification factors

The calibration factor c of an ion with a arbitrary mass to charge ratio for a given setting of VMI voltages from Table 1 can be described:

$$c = \frac{1}{\text{magnification factor}} \frac{\text{TOF}_{m=53u}}{\text{TOF}_{ion}} \frac{1 \text{ mm}/\mu\text{s}}{9 \text{ pixel}} \quad (2)$$

where TOF_{ion} is the time of flight of the arbitrary ion. The calibration factor c represents the ratio of the radial detector position in pixel to the radial start position in mm for spatial imaging and the ratio of the radial detector position in pixel to the radial start velocity in $\text{mm}/\mu\text{s}$ for velocity imaging.

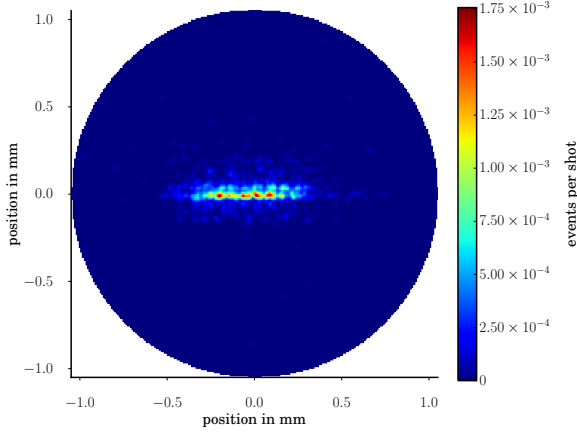


Figure 7: Spatial image slice of molecular beam

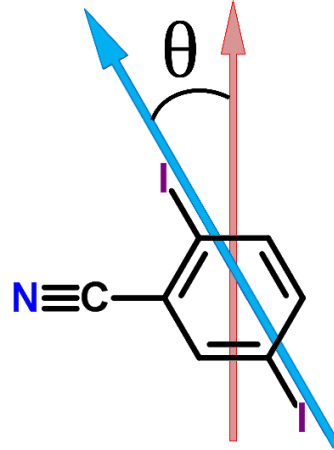


Figure 8: Definition of angle θ ,
red: elec. field of alignment laser
blue: most-polarizable DIBN axis

3.2 Spatial Imaging

In spatial imaging the positions of birth of the ions is pictured to detector positions. Two ions starting at the same point also arrive at exactly the same point of the image, independent of their initial velocities. Figure 7 is a spatial projection of the ions which are created on the probe laser's horizontal path through the molecular beam. The molecular beam propagates perpendicularly to the image plane in this picture.

3.3 Velocity Map Imaging

In velocity imaging only the start velocities of the ions are pictured to a detector position, so that the image represents the projection of the initial velocity vectors on the detector. Even if ions differ in their initial position they are mapped at the same point of the image in case of same velocity vectors.

Figure 9 shows the impact of the alignment laser on the velocity map image. Figure 9 (a) shows a isotropic distribution of I^+ ions. The degree of alignment can be expressed by $\langle \cos^2 \theta \rangle_{2D}$ which is defined as:

$$\langle \cos^2 \theta \rangle_{2D} = \int_0^{2\pi} \int_{v_1}^{v_2} \cos^2(\theta) f(\theta, v) d\theta dv \quad (3)$$

with the angle θ between the ion velocity vector and the polarization of the alignment laser (Figure 8) and the ion distribution $f(\theta, v)$ on the detector. All angles and velocities used in this equation are the two dimensional projections on the detector. $\langle \cos^2 \theta \rangle_{2D}$ equals 0.5 for a perfect random distribution and becomes 1 for ideal alignment.

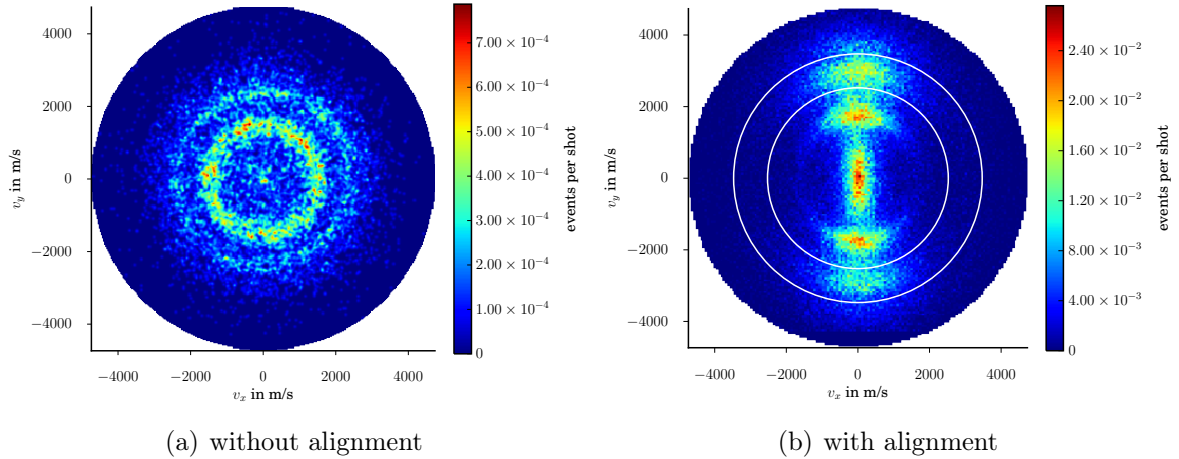


Figure 9: Velocity maps of I^+ from DIBN

For Figure 9 (a) we get $\langle \cos^2 \theta \rangle_{2D} = 0.51$ which is close to the expected value of $\langle \cos^2 \theta \rangle_{2D} = 0.5$ for a perfect isotropic distribution. Figure 9 (b) shows a velocity map using the alignment laser. One can see some counts in the center with almost no initial velocity and two discrete fragmentation channels at around 1700 m/s and 3000 m/s

which are both I^+ ions from different Coulomb explosion channels. It is preferable to use just the outer channel to calculate the degree of alignment because the faster ions represent the orientation of the molecules in a better way. Large velocities indicated the removing of many electrons at the strong-field ionization making it probable that both iodine ions were polarized and fled apart in opposite directions. After the alignment pulse the molecules can start to rotate again which has a higher effect on slow flying ions. Just considering the counts in between the two white circles we get $\langle \cos^2\theta \rangle_{2D} = 0.842$ for Figure 9 (b). The intensity scales differ from each other in Figure 9 (a) and (b) h, because alignment increases the contrast of the picture.

Figure 10 (a) depicts the radial distribution of the velocity map with alignment, where one can easily find the velocity of both ionization channels. Figure 10 (b) visualizes the alignment through an angular distribution.

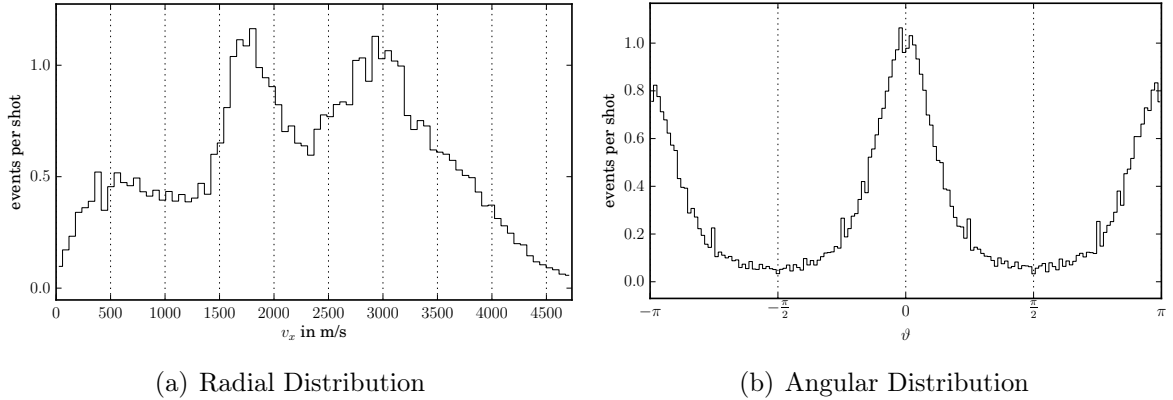


Figure 10: Image analysis of aligned velocity map (Figure 9 (b))

4 Measurement

4.1 Time Offset

The time frame when the MCP was collecting data was determined by a high-voltage switch with nanosecond rise time. Thus one could select the time of flight, when a fragment with a certain mass m to charge number Z ratio $R = \frac{m}{z}$ arrived at the detector. This time frame could be basically set according to the simulated time of flight of the particular ions of interest. Moreover we had to add a time offset due to the electronics to the time setting. The TOF measurement of two different ions was needed to calculate this time offset with the following formula, assuming same kinetic energies for both ions, when they arrived at the detector.

$$t_0 = \frac{t_2 \cdot \sqrt{\frac{R_1}{R_2}} - t_1}{\sqrt{\frac{R_1}{R_2}} - 1} \quad (4)$$

Using the measured time of flights of H_2O^+ ($t_1 = 1.5482 \mu\text{s}$) and He^+ ($t_2 = 0.9134 \mu\text{s}$) and their corresponding masses, the calculated offset of the setup could be determined to $t_0 = 347 \text{ ns}$.

4.2 Beam Profile

Figure 7 shows a cut through the molecular beam. By changing the position of the laser lens and thereby the vertical laser position one could make many slices of the molecular beam. The scan of the whole beam profile is shown in Figure 11. Not the full circular molecular beam is pictured, because the upper part of the beam was cut away by the rod of the deflector. To avoid this disadvantage for strong deflection there is current research on deflectors with a different geometry to avoid beam cutting.

Fitting a Gaussian curve to the uncut part of the vertical beam profile (Figure 12 (a)) gave a standard deviation of $\sigma = 0.53 \pm 0.01 \text{ mm}$. Therefore the vertical $1\text{-}\sigma$ interval had a size of $1.06 \pm 0.02 \text{ mm}$ which is what we expected for the size of our beam.

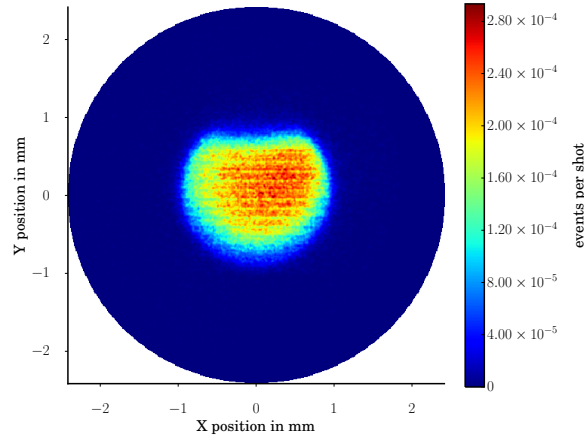


Figure 11: Beam Profile

This standard deviation could be also used to calibrate the spatial axes because we already calibrated the laser position. By comparing 1D and 2D Gaussian fit of the one dimensional cut with the two dimensional map of the same image (Figure 12 (b)), one got a calibration factor of 0.0105 mm/pixel in between the spatial coordinates of the molecular beam and pixels of the camera.

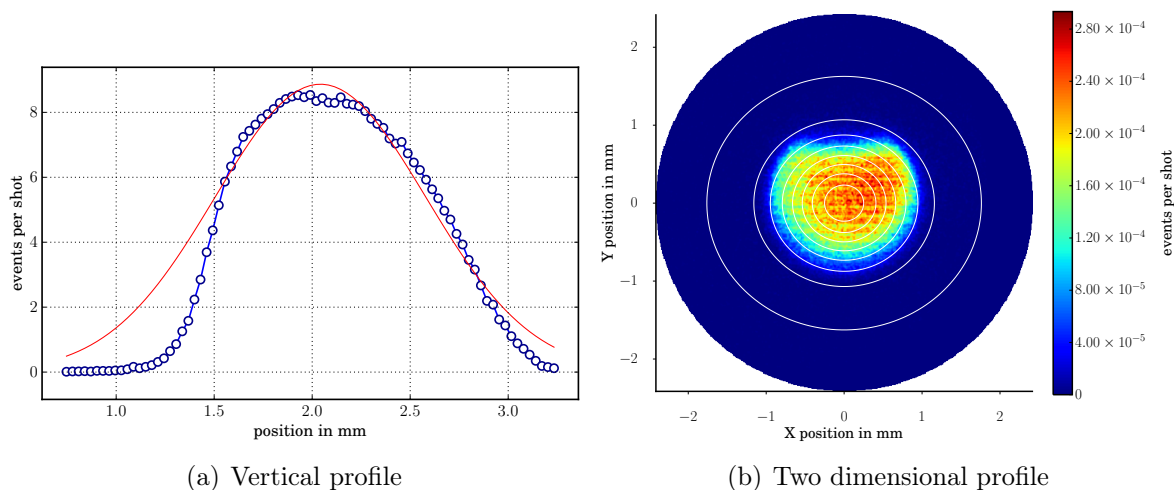


Figure 12: Gaussian Fit of 1D and 2D beam profile

5 Conclusion

In conclusion, an experimental setup for imaging controlled molecules was described. We were able to control DIBN up to a degree of alignment of $\langle \cos^2\theta \rangle_{2D} = 0.842$. This will allow to measure electron diffraction in the future to investigate molecular structure. To get started, in particular iodine-containing species are useful for diffraction because they have many electrons to diffract off and I-I-axes are easy to polarize and align. Later on the aim is to investigate the structures of any molecule during dynamic changes to produce molecular movies and get a more precise understanding of chemical reactions and processes.

Acknowledgment

I would like to thank my supervisor Joss Wiese and Nele Müller for their time, helpful advices and the inspiring time of research. Moreover I want to thank the organization team of the DESY Summer Student Program.

References

- [1] Christopher J. Hensley, Jie Yang, and Martin Centurion, *Imaging of Isolated Molecules with Ultrafast Electron Pulses*, Phys. Rev. Lett. **109**, 133202.
- [2] Sebastian Trippel, Terry Mullins, Nele L. M. Müller, Jens S. Kienitz, Karol Długołęcki, and Jochen Küpper, *Strongly aligned and oriented molecular samples at a kHz repetition rate*, Mol. Phys. **111**, 1738-1743 (2013), arXiv:1301.1826 [physics].
- [3] Nele L. M. Müller, Sebastian Trippel, Karol Długołęcki, and Jochen Küpper, *Electron gun for diffraction experiments off controlled molecules*, arXiv:1507.02530v2 [physics].
- [4] Henrik Stapelfeldt and Tamar Seideman, *Colloquium: Aligning molecules with strong laser pulses*, Rev. Mod. Phys. **75**, 543 (2003).
- [5] Andre T. J. B. Eppink and David H. Parker *Velocity map imaging of ions and electrons using electrostatic lenses: Application in photoelectron and photofragment ion imaging of molecular oxygen*, Review of Scientific Instruments **68**, 3477 (1997).
- [6] D. A. Dahl, J. E. Delmore, and A. D. Appelhans *SIMION PC/PS2 electrostatic lens design program*, Rev. Sci. Instrum. **61**, 607 (1990)
D. Manura, D. Dahl. SIMION ®8.0 User Manual (Scientific Instrument Services, Inc. Ringoes, NJ 08551, <http://simion.com>, September 2015).